WIDEBAND DIGITAL SIGNAL PROCESSING TEST-BED FOR RADIOMETRIC RFI MITIGATION

Damon C. Bradley, Adam J. Schoenwald, Mark Wong, Priscilla N. Mohammed, Jeffrey R. Piepmeier

NASA Goddard Space Flight Center, Greenbelt, Maryland

ABSTRACT

RFI is a persistent and growing problem experienced by spaceborne microwave radiometers. Recent missions such as SMOS, SMAP, and GPM have all detected RFI in L, C, X, and K bands. To proactively deal with this issue, microwave radiometers must include digital back-end processors that generate data products that facilitate the detection and excision of RFI from desired brightness temperature measurements. The wideband digital signal processing testbed is a platform that allows rapid development of various RFI detection and mitigation algorithms using digital hardware akin to that which might be used for final spaceflight implementation. On it, we evaluate an improved version of the SMAP RFI Digital Signal Processor (DSP) that utilizes the new complex signal kurtosis algorithm as opposed to the real signal kurtosis that is used on the SMAP radiometer. In addition, we show how we scale the DSP to operate at 8.3 times the bandwidth of the SMAP radiometer for operation in K-band.

Index Terms— Interference, Circularity, Complex Random Process, Radiometer, Digital Receiver, SERDES

1. INTRODUCTION

To address the problem of RFI, particularly for L-band radiometers, many researchers have developed RFI detection and mitigation methods that utilize a diverse array of signal processing tools, such as the spectrogram, pulse-blanking, higher-order statistics, cross-correlation of polarimetric radiometer channels, complex-valued statistical signal processing, and information-theoretic algorithms [1–4]. With the availability of fast sampling analog to digital converters (ADCs) and Field-Programmable Gate Arrays (FPGAs), sophisticated radiometer DSP systems can be implemented that use any combination of these algorithms, such as the Soil Moisture Active Passive Mission (SMAP) [5].

At higher Earth Science frequency allocations with wider bandwidth, such as K-band (18.6 − 18.8 GHz), RFI is also problematic [6]. Not only do systems operating at these frequency bands have bandwidths that are an order of magnitude wider than those at L-band, but they also share spectrum with active services that cause RFI [7]. As a result, there are new signal processing challenges that arise when implementing RFI mitigation subsystems that differ from implementation at the smaller bandwidth of L band.

To evaluate and address these challenges for RFI mitigation at K-band, a 1 GHz sample-rate polarimetric radiometer test-bed was developed at NASA Goddard Space Flight Center using the Reconfigurable Open Architecture Computing Hardware (ROACH) system from the Collaboration for Astronomy Signal Processing and Electronics Research (CASPER) group at the University of California Berkeley (Figure 1). The CASPER-ROACH system is a convenient development platform since it operates over 1 GHz for multiple signal channels, it leverages a large library of community provided intellectual property (IP) blocks, and utilizes the Matlab-Simulink model-based design framework. This allows for an increased focus on algorithm development as opposed to FPGA design, and facilitates rapid prototyping and evaluation of newly developed RFI mitigation techniques.
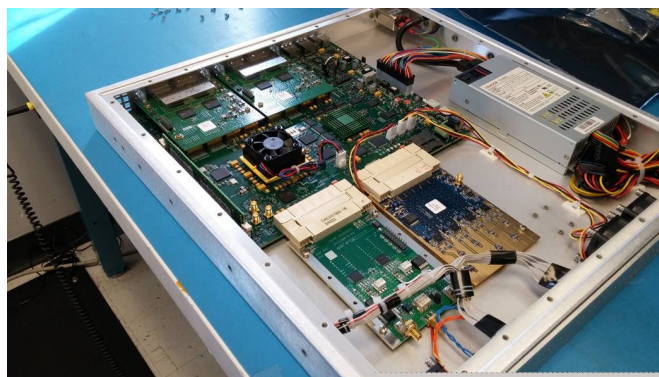
Fig. 1. CASPER-ROACH FPGA-based DSP platform used for evaluating new RFI mitigation techniques.

In this paper, we discuss new techniques for RFI mitigation processing that we implemented on the CASPER-ROACH system. First, we implemented the new *complex signal kurtosis* (CSK) algorithm [8]. Second, we demonstrate a scaled version of the SMAP radiometer DSP to operate at 8.3 times its bandwidth for K-band as opposed to L-band operation. We discuss how operation at K-band requires a modification in the SMAP RFI processor, and how the mod-

ified SMAP RFI processor that uses the CSK algorithm for RFI detection can achieve better receiver operating characteristic (ROC) performance and reduce data rate to the ground at the same time.

2. COMPLEX SIGNAL KURTOSIS ALGORITHM

From a hardware standpoint, the first issue to address for a DSP system that performs RFI mitigation processing is data rate. In the case of SMAP radiometer, although the radiometric bandwidth used is 24 MHz, it is necessary to sample the pre-detected radiometric signal at 96 MHz. As a result, we can maximally decimate the data by a factor of 4 and not compromise the information bandwidth. Decimation requires a digital downconverter (DDC) and the lowest possible data rate is achievable when the input signals are downconverted to a complex baseband in-phase and quadrature (I/Q) representation in hardware. For K-band, decimation is even more important since FPGAs that perform the processing simply cannot operate at the signal sample rate. Data rate reduction via downconversion and decimation has to be built into the data acquisition architecture of a K-band system.

The issue that arises when downconverting to complex baseband is that one is left with an N-sample complex signal, $z(n) = I(n) + jQ(n), n \in [0, \ldots, N-1]$ for each polarization component channel. N corresponds to the number of time samples in a single radiometric integration period τ, at sample rate F_S. Therefore $N = \lceil \tau F_S \rceil$. All signal sample moments that are required for radiometry (mean and variance) and RFI mitigation (variance, skewness, kurtosis) must therefore use moments of a complex random variable as opposed to a real random variable as is customarily done. Using the definition in [9] and dropping the time index n, the $p(= \ell + m)$th-order sample central moment of this signal is defined by

$$\alpha_{\ell,m} = \mathbb{E}\left[(z - \mathbb{E}[z])^\ell (z - \mathbb{E}[z])^{*m}\right], \quad \ell, m \in \mathbb{Z}_{\geq 0}, \quad (1)$$

where $\mathbb{E}$ is the expectation operator and $*$ is the complex conjugate. *Standardized moments* are defined by

$$\varrho_{\ell;m} = \frac{\alpha_{\ell,m}}{\sigma^{\ell+m}}, \quad (2)$$

where $\sigma^2 = \alpha_{1,1}$. Since $\alpha^*_{\ell,m} = \alpha_{m,\ell}$, there are three unique kurtosis definitions for a complex signal. These are called *kurtosis coefficients* $\gamma_{4;0}$, $\gamma_{3;1}$, and $\gamma_{2;2}$ — defined in [9] which also derived a test-statistic

$$C_K = \frac{\gamma_{2;2}}{1 + \frac{1}{2}|\varrho_{2;0}|^2} \cdot \quad (3)$$

where $\gamma_{2;2}$ is a real-valued measure of the complex signal kurtosis and defined by

$$\gamma_{2;2} = \varrho_{2;2} - 2 - |\varrho_{2;0}|^2. \quad (4)$$

If $z(n)$ is Gaussian, then $C_K = 0$. Otherwise, C_K is nonzero. Therefore C_K is a test statistic for non-Gaussianity that can be used for RFI detection. The test statistic in (3) was implemented on the CASPER-ROACH system, replacing the statistics calculation unit used in the SMAP radiometer DSP.

3. ROC PERFORMANCE OF CSK ALGORITHM

The SMAP radiometer DSP computes all moments of the in-phase and quadrature component signals separately and then combines them in ground processing to make the RFI test statistic

$$R_K = \frac{kurt\{I(n)\} + kurt\{Q(n)\}}{2} \quad (5)$$

where $kurt\{\cdot\}$ is the real signal kurtosis $\mathbb{E}\left[(y - \mathbb{E}[y])^4\right]/\sigma^4$, $y(n)$ is either $I(n)$ or $Q(n)$, and σ^2 is the sample variance of y. The CSK, however, uses the normalized complex signal kurtosis C_K, which operates on $I(n)$ and $Q(n)$ together as a single complex-valued signal.

To evaluate the RFI detection performance of C_K vs. R_K, two Monte-Carlo simulations were performed using an additive RFI signal model

$$x(n) = w(n) + s(n), \quad (6)$$

where $x(n)$ is pre-detected radiometer signal, $z(n)$ is the baseband complex version of this signal, $s(n)$ is the RFI signal model, and $w(n)$ is unit-variance Gaussian white noise. For $s(n)$ we used the single-sinusoidal interferer model

$$s(n) = A\cos\left(2\pi f_0 n/F_S\right) \Pi\left(n\right). \quad (7)$$

With signal parameters of amplitude, frequency, and duty cycle A, f_0, and d, sample rate F_S, and rectangle function $\Pi(n)$ with duty-cycle d. We differentiated between continuous-wave (CW) where $d = 100\%$ and pulsed-continuous Wave (PCW) where $d < 100\%$ for each simulation, respectively. All parameters of the RFI model in the first Monte-Carlo simulation were fixed except the amplitude. In the second, all model parameters were fixed except duty cycle. The resulting Figures 2 and 3 show ROC curves and corresponding areas under the curve (AUC) for different parameter values for A and d, respectively. In all cases, the CSK outperforms the R_K detection algorithm. This result suggests that not only CSK algorithm better for detecting RFI than R_K, it also implies that $I(n)$ and $Q(n)$ can be combined on the radiometer DSP in space, as opposed to transmitting down separate statistics for the $I(n)$ and $Q(n)$ signals. This reduces the instrument to ground data rate by a factor of 2.

4. K-BAND RADIOMETER DSP ARCHITECTURE

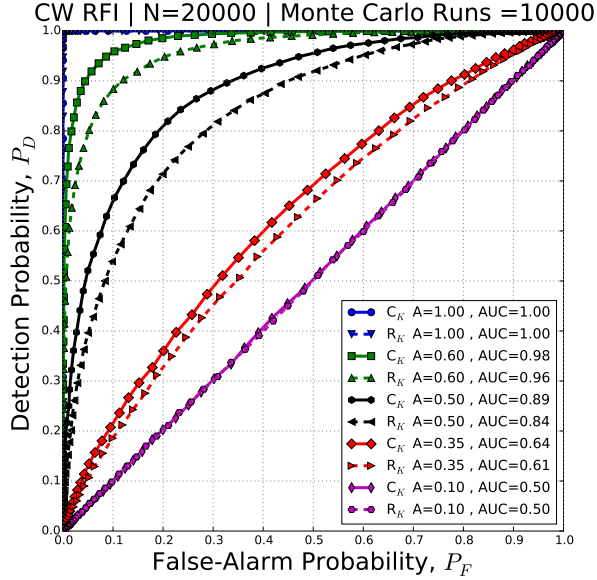To process digitally sampled data from a radiometer, ADCs with high sample rates ($F_S > 100$ MHz) must be used and

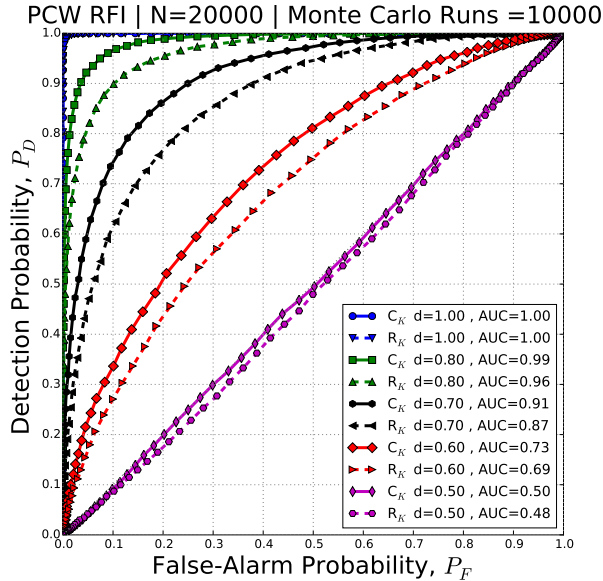**Fig. 2**. ROC for various CW interference types, parametrized by SNR.

Fig. 3. ROC for various Pulsed-CW interference types, parametrized by SNR.

interfaced directly with an FPGA that can ingest the data volume. FPGAs however, operate at maximum switching frequency F_{MAX} that is a function of the device family, operating temperature, total logic utilization, and quality of design. When $F_S < F_{MAX}$, the ADC can provide the digitized signal directly to the FPGA pins and subsequent digital logic. The digital logic can then implement the RFI signal processing stages serially, as in [10], for example. Conversely, if $F_S > F_{MAX}$, the digitized signal must first be split into two or more parallel processing paths so that the effective clock switching rate of each path is less than F_{MAX}. This process is called *serialization-deserialization* or SERDES. SERDES is required to acquire digital signals from ADC's that sample faster than the FPGA F_{MAX}.

For K-band operation, since the radiometric bandwidth allocation is 200 MHz, ADCs that can sample greater than 400 MHz are required. However, this rate far exceeds the F_{MAX} of any FPGA used for spaceflight, so SERDES must be used in the FPGA. The use of SERDES requires parallelization of portions of the subsequent algorithm since it is operating with the serial input signal split across multiple data paths in parallel.

When migrating the SMAP DSP design to the CASPER-ROACH system, only the DDC needs to be parallelized if decimation is used in the RFI processing algorithm. SMAP used an efficient serialized version of a polyphase DDC that operated at $F_S/4$. It was found that this downconverter could be deserialized into its theoretical form to operate on the SERDES data. The remaining processing pipeline could be maintained.

The modified SMAP SERDES DDC was combined with the CSK algorithm to produce a complete radiometer digital back-end that generates a $C_K^{(\ell)}$ RFI test-statistic for every signal variance $\sigma_{(\ell)}^2$ estimate used for brightness temperature measurement (Figure 4). The CSK algorithm is applied to every channel of the polyphase filterbank (PFB) ℓ, allowing RFI to be detected by the CSK algorithm in the time-frequency cells of the resulting spectrogram output of the system. Compared with the SMAP radiometer DSP implementation of 24 MHz bandwidth, this system can operate with 200 MHz of bandwidth, representing a scaling factor of 8.3.

5. CONCLUSIONS AND FUTURE WORK

The Wideband DSP Test-Bed using the CASPER-ROACH system was successfully implemented as a platform for evaluating RFI detection algorithms for K-band RFI. The new CSK algorithm was implemented on this system, along with a high-data rate modification to the SMAP radiometer DSP processor. It was shown that to upgrade the current SMAP algorithm to be applicable in K-band, the DDC needed to be parallelized to handle the faster data rate. Downconversion to complex baseband was also necessary to reduce the data rate, and the CSK algorithm was developed to reduce data
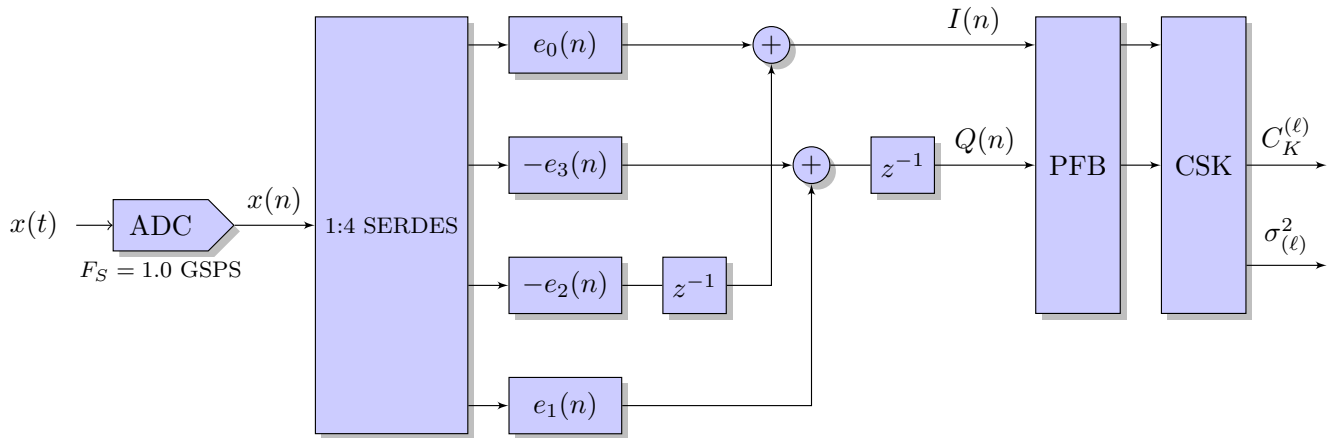
Fig. 4. Architecture of Wideband RFI Processor using a SERDES/Polyphase DDC architecture and CSK detector for each filterbank channel. DDC image rejection filter is split into 4 polyphase subfilters $e_1(n), \ldots, e_4(n)$. Mixing, image filtering, and decimation by 4 are all integrated into the polyphase FIR filter.

rate further while improving RFI detection performance. In the future, we plan to increase the number of filterbank channels in the system and explore the use of $\varrho_{4;0}$ and $\varrho_{3;1}$ for RFI detection.

6. REFERENCES

[1] D. Bradley and J. Morris, "On the performance of negentropy approximations as test statistics for detecting sinusoidal RFI in microwave radiometers," *IEEE Transactions on Geoscience and Remote Sensing*, vol. 51, no. 10, pp. 4945–4951, October 2013.

[2] S. Misra, P. Mohammed, B. Guner, C. Ruf, J. Piepmeier, and J. Johnson, "Microwave radiometer radio-frequency interference detection algorithms: A comparative study," *IEEE Transactions on Geoscience and Remote Sensing*, vol. 47, no. 11, pp. 3742 –3754, November 2009.

[3] B. Güner, N. Niamsuwan, and J. Johnson, "Performance study of a cross-frequency detection algorithm for pulsed sinusoidal RFI in microwave radiometry," *IEEE Transactions on Geoscience and Remote Sensing*, vol. 48, no. 7, pp. 2899 –2908, July 2010.

[4] N. Skou, S. Misra, J. Balling, S. Kristensen, and S. Sobjaerg, "L-band RFI as experienced during airborne campaigns in preparation for SMOS," *IEEE Transactions on Geoscience and Remote Sensing*, vol. 48, no. 3, pp. 1398–1407, 2010.

[5] J. Piepmeier, J. Johnson, P. Mohammed, D. Bradley, C. Ruf, M. Aksoy, R. Garcia, D. Hudson, L. Miles, and M. Wong, "Radio-frequency interference mitigation for the soil moisture active passive microwave radiometer," *IEEE Transactions on Geoscience and Remote Sensing*, vol. 52, no. 1, pp. 761–775, January 2014.

[6] D. McKague, J. J. Puckett, and C. Ruf, "Characterization of K-band radio frequency interference from AMSR-E, WindSat and SSM/I." in *IGARSS'10*, Honolulu, HI, USA, July 2010, pp. 2492–2494.

[7] Committee on Scientific Use of the Radio Spectrum; Committee on Radio Frequencies; National Research Council, *Spectrum Management for Science in the 21st Century*. The National Academies Press, 2010.

[8] D. Bradley, J. M. Morris, T. Adali, J. T. Johnson, and A. Mustafa, "On the detection of RFI using the complex signal kurtosis in microwave radiometry," in *to appear in 13th Specialist Meeting on Microwave Radiometry and Remote Sensing of the Environment (MicroRad) 2014*, Pasadena, CA, USA, March 2014.

[9] E. Ollila, J. Eriksson, and V. Koivunen, "Complex elliptically symmetric random variables - generation, characterization, and circularity tests." *IEEE Transactions on Signal Processing*, pp. 58–69, December 2011.

[10] D. Bradley, C. Brambora, M. Wong, L. Miles, D. Durachka, B. Farmer, P. Mohammed, J. Piepmier, J. Medeiros, N. Martin, and R. Garcia, "Radio-frequency interference (RFI) mitigation for the soil moisture active/passive (SMAP) radiometer," in *Geoscience and Remote Sensing Symposium (IGARSS), 2010 IEEE International*, Honolulu, HI, USA, July 2010, pp. 2015 –2018.